

FILE COPY

Columbia University
in the City of New York

LAMONT GEOLOGICAL OBSERVATORY
PALISADES, NEW YORK

7-10-29

Technical Report on Seismology No. 23

[Contract Report No. 22]

An Investigation of Mantle Rayleigh Waves

LAMONT GEOLOGICAL OBSERVATORY

(Columbia University)

Palisades, New York

* * *

Technical Report No. 23

An Investigation of Mantle Rayleigh Waves

by

Maurice Ewing and Frank Press

The research reported in this document has been made possible through support and sponsorship extended by the Geophysics Research Division of the Air Force Cambridge Research Center under Contract AF19(122)441. It is published for technical information only and does not represent recommendations or conclusions of the sponsoring agency.

September 1952



Digitized by the Internet Archive
in 2020 with funding from
Columbia University Libraries

<https://archive.org/details/investigationfm00ewin>

ABSTRACT

Dispersion of Rayleigh waves for a new range of periods ranging from 1-7 minutes is described. The group velocity curve shows a long period and short period branch merging at a minimum value of 3.54 km/sec with a corresponding period of about 225 sec. It is suggested that the known variation of velocity with depth in the mantle can account for the observed dispersion. The small scatter in the velocities and the absorption of these waves suggests that unlike microseisms, refraction and attenuation effects are negligible at the continental margins. From the absorption of mantle Rayleigh waves the internal friction in the upper mantle for periods of 140 and 215 sec is found to be given by $1/Q = 670 \times 10^{-5}$. This is of the same order as that reported from vibration measurements at audio frequencies on laboratory samples of crystalline rocks at normal pressure and temperature.

INTRODUCTION

The present study of the Rayleigh waves in the period range 1-7 minutes was made possible through the cooperation of Prof. H. Benioff who brought the author's attention to the long Rayleigh waves recorded at Pasadena for the three earthquakes considered. The first of these is the great Assam earthquake of 15 August 1950. According to B.C.I.S. the epicenter is 28.6°N 96.5°E , origin time 14:09:30. The Pasadena magnitude was 8.6, epicentral distance 109.5° and azimuth of the epicenter $\text{N}32^{\circ}\text{W}$. The Rayleigh waves R3, R4, R5, R7, which B. Gutenberg had reported in the Pasadena Bulletin, were read for a wide range of periods on the long period Benioff vertical and North-South seismographs and on the North-South linear strain seismograph. The second earthquake was the Japanese shock of 2 March 1933. According to I.S.S. the epicenter is 39.1°N , 144.7°E , origin time 17:31:01. The Pasadena magnitude was 8.5, epicentral distance 74.1° and azimuth of the epicenter $\text{N}58^{\circ}\text{W}$. The Rayleigh waves R2, R3, R4 were read on the N-S linear strain seismograph. The third earthquake studied was the Tonga shock of 8 September 1948 which according to J.S.A. occurred at 21.0°S , 174.2°W , origin time 15:09:14. The Pasadena magnitude was 8, epicentral distance 76.8° , and azimuth of the epicenter $\text{S}53^{\circ}\text{W}$. Only R2 could be read

for this earthquake on the long period Benioff vertical seismograph.

Although the paths of the Rayleigh waves involve as much as three complete passages around the earth, the orbital motion of a surface particle could be demonstrated to be proper for Rayleigh waves and the group velocities deduced from all the paths could be represented by a single dispersion curve whose broad features may be accounted for in terms of mantle structure.

The investigation of Rayleigh wave dispersion in the period range 1 to 7 minutes represents a new field of study, for most previous studies have been devoted to waves with periods less than about 50 sec. Many writers have made deductions of crustal structure from the observed Rayleigh wave dispersion curves, and the general conclusion is that the sialic rocks of the continents extend to a depth of about 40 km, and that they are essentially absent under the oceans. Wilson and Baykal¹ have presented the most recent dispersion curve for continents covering the period range 16 to 28 seconds. Ewing and Press² have presented dispersion curves for purely oceanic paths covering the period range 14 to 38 seconds, with velocities becoming less than half as large as those for the

1. J. T. Wilson and Orhan Baykal, "Crustal Structure of the North Atlantic Basin as Determined from Rayleigh Wave Dispersion", Bull. Seism. Soc. Amer., 38, 41-53, 1948.

2. Maurice Ewing and Frank Press, "Crustal Structure and Surface Wave Dispersion Part II, Solomon Islands Earthquake of 20 July 1950, in press Bull. Seism. Soc. Amer.

4.

continents for some periods. The whole oceanic dispersion curve was quantitatively accounted for by allowance for the effect of the water layer on Rayleigh waves propagated in the underlying simatic rock.

The great contrast between continental and oceanic dispersion for periods less than one minute accounts for the bewildering variety of dispersion curves and the corresponding variety of general patterns of surface waves which have been obtained from mixed paths involving varying proportions of continental and oceanic segments. This contrast likewise causes strong effects of refraction and scattering at continental boundaries, thereby insuring that waves of periods less than one minute will be very weak, or absent for paths such as the R2, R3, R4 and R7 which involve one or more complete trips around the earth and in general, many passages across continental boundaries.

We consider that the short period limit of 1 minute for the long period waves is imposed by crustal structure, being the shortest wave length for which the continental and oceanic dispersion curves show no appreciable difference. The long period limit of about 7 minutes is probably imposed by the seismometers, and seismometers capable of recording waves of longer period may be expected

to carry Rayleigh wave observations to the point where gravity and sphericity terms must be included and where the dimensions and properties of the core may be investigated.

DATA

In Figure 1 tracings of the Pasadena long period vertical and N-S ($T_0=1$ sec $T_g=90$ sec) and N-S linear strain ($T_g=70$ sec) seismograms are presented for the earthquake of 15 August 1950. The maximum and minimum deflections were read for R3, R4, R5 and R7. A deflection on the vertical component seismogram in the direction marked "ground up" relates to the response to an impulsive upward ground movement, as is customary. The same convention is followed for the North-South and for the linear strain seismograms. For all readings made from these seismograms the waves are approximately sinusoidal and with a minor exception the periods are well above those for the pendulums or galvanometers. Since the transducers and galvanometers are identical for all three instruments one can discuss the phase relations by simply noting that the response of the pendulum is proportional to ground acceleration whereas the strain instrument responds directly to compressional and rarefractional strain.

Hence maximum trace deflections on each of the three instruments bear the same phase relationship as "ground down", "ground south", and "compression". For this reason ground motion

corresponding to maximum trace deflection on the vertical, horizontal and N-S strain seismographs will be denoted by D, S, C respectively and minimum trace deflections will be denoted by U, N, R.

Tables 1 to 4 give uncorrected arrival times for the maximum and minimum trace deflections indicated for the earthquake of 15 August 1950. Corrected time may be obtained by adding 23 seconds. It will be noted that the orbital motion, as indicated by the sequence of readings, is proper for Rayleigh waves from the north in the case of R3, R5, and from the south for R4. R7 could be read only on the vertical.

The arrival time curves for the various orders of Rayleigh waves are shown in Figs. 2, 3, 4, and 5. The abscissas are arrival times, and the ordinates to the left represent the phase of the oscillations, one space representing one-half cycle. The small arrows represent the limits of the straight line segments with which each curve was approximated. The slope and mid-point of each straight line segment were read from these graphs, and from them the arrival times for waves of each period were computed. These results are plotted on the same graphs as period curves. Travel time and group velocity was then computed for each period. The resulting dispersion data for each order of Rayleigh waves appears in Table 5.

It will be noted that each of these arrival time and period curves (except R7) has first a long period branch, representing a train of waves whose period decreases with time. The long period branch is interrupted abruptly by a train of much shorter waves in which the period increases with time. In many cases it is possible to read the long period waves for several cycles following the onset of the short period waves, but as is usual when working near a minimum value of group velocity, one cannot read both branches to the point where the periods are equal. This gap in readings might suggest that there is arbitrary choice in fitting the ordinates of each short period branch of the arrival time curves to the long period branches, but the gap is too short to permit uncertainty.

Arrival times for maximum and minimum trace deflections of R2, R3, R4 waves are plotted in Table VI for the earthquake of 2 March 1933. Dispersion data is given in Table VII. Table VIII gives the corresponding data for R2 waves from the earthquake of 8 September 1948. These data are depicted in graphical form in Figures 6, 7. Group velocity as a function of period for all observed orders of Rayleigh waves is presented in Figure 8. The dotted part of the curve represents the portion which is unobservable, due to the overlapping of the two branches. It is easily seen that the choice of ordinates in Figures 2, 3, 4 which was made produces a reasonable

shape for the dotted part of the dispersion curve, which is demanded by the character of R7.

It can be seen that a single dispersion curve represents all the orders and that there is no indication whatever of a systematic shift of this curve with increasing length of path. It is also evident that the spectra of the various Rayleigh wave trains are determined primarily by dispersion since R3, R5 and R7 cover progressively narrower period ranges centering about 225 sec, the period for minimum group velocity. This agrees with the well-known relation between amplitude and the slope of the group velocity curve. Analogous results have been obtained in propagation of explosion sounds in shallow water.³

For the earthquake of 15 August 1950 R4 was observable for a period range almost as long as that for R3. This probably results from the fact that the seismogram in the neighborhood of R3 is still considerably disturbed by short period surface waves, but the possibility of an azimuthal dependence cannot be entirely ruled out. Observations of R6 would have settled this point, but unfortunately the seismograms are unreadable during the interval 22:09 to 22:50 due to artificial disturbance.

3. M. Ewing, J. L. Worzel, C. L. Pekeris, "Propagation of Sound in the Ocean", Geol. Soc. Amer., Mem. 27, 1948.

The remarkable agreement of the dispersion for the various orders of Rayleigh waves suggests that scattering effects are negligible in the propagation of mantle Rayleigh waves. Absorption studies on these waves should yield data on elastic imperfection in the mantle with a higher degree of precision than was available in earlier investigations of shorter period waves where scattering could not be estimated. Earlier investigations suffer from the added difficulty that waves of a given period could not be followed over the wide range of distances available in this study.

AMPLITUDES

In Tables I-IV peak to peak ground amplitudes are listed as a function of arrival time for the short period branches of R3, R4, R5, R7 waves from the earthquake of 15 August 1950. These data along with periods are plotted as a function of arrival time in Figures 2, 3, 4, 5. From these graphs ground amplitudes were obtained as a function of period, the data appearing in Table IX, and plotted in Figure 9. It is seen that the maximum amplitudes fall between 205 and 225 seconds, reasonably close to the period of minimum group velocity. Amplitudes could be read with precision only for these waves, the relatively high background preventing similar treatment for the long period branch and for the waves from the other shocks.

Since the effect of geometrical spreading is a constant for the various orders of Rayleigh waves, at a given station the amplitude for the Airy phase will vary approximately as $e^{-\gamma\Delta/\Delta'^{1/3}}$. In a similar manner the amplitude for any other period in the wave train will vary as $e^{-\gamma\Delta/\Delta'^{1/2}}$. Here γ represents the loss due to dissipation effects and the factors $\Delta^{1/3}$ and $\Delta'^{1/2}$ represent the effect of dispersion or "stretching" of the wave train. The exponents of Δ given above ignore an effect of sphericity but are considered satisfactory for an approximate calculation. Although not needed for study of a single station, approximate allowance for the effect of geometrical spreading is made by the factor $(r_0 \sin \Delta)^{-1/2}$, where r_0 is the earth's radius, except for Δ near to $0, \pi, 2\pi$ etc.

Thus we will use the relations

$$A = \frac{\bar{A}_0 e^{-\gamma\Delta}}{|r_0 \sin \Delta|^{1/2} \Delta^{1/3}} \quad |$$

for the Airy phase and

$$A = \frac{A_0 e^{-\gamma\Delta}}{|r_0 \sin \Delta|^{1/2} \Delta'^{1/2}} \quad 2$$

for other periods in the wave train.

From the amplitude vs. period curves of Figure 9 the constants A_0 and γ are readily determined for a given period by making a plot of $\ln(A \cdot \Delta'^{1/3})$ against Δ for the Airy phase or $\ln(A \cdot \Delta'^{1/2})$

12.

for the other waves. Such a graph is presented in Figure 10. It is seen that the data for $T=140$ sec, 180 sec, and 215 sec (Airy phase) can be represented by the two straight lines indicated. These lines give the relations

$$A_z = \frac{104}{\Delta'^{\frac{1}{2}}} e^{-0.0024\Delta} \quad \text{for } T=215 \text{ sec} \quad 3$$

and

$$A_z = \frac{144}{\Delta'^{\frac{1}{2}}} e^{-0.0040\Delta} \quad \text{for } T=140 \text{ sec.} \quad 4$$

The absorption coefficients $.0024 \text{ degrees}^{-1}$ ($.0000216 \text{ km}^{-1}$) and $.0040 \text{ deg}^{-1}$ ($.0000360 \text{ km}^{-1}$) thus determined show that the amplitudes of mantle Rayleigh waves decrease by two fifths for $T=215$ sec and by one fourth for $T=140$ sec due to absorption alone for each circuit of the earth.

A simple computation indicates that if viscosity is to account for the absorption a value of the order of $10^{15} - 10^{16}$ poises is needed in the upper mantle. Since this is many orders of magnitude less than the values $10^{20} - 10^{22}$ poises given by the occurrence of deep focus earthquakes and the recoil of the earth after the disappearance of the Pleistocene ice in Fennoscandia⁴, the absorption can be ascribed

4. "Internal Constitution of the Earth", Chapter XV, Sec. Ed., Dover Publications, New York, 1951.

to the effect of internal friction.

The internal friction may be specified by a dimensionless parameter Q^5 related to the absorption coefficient γ by the equation

$$\gamma = \pi / Q c T$$

5

where c is phase velocity and T is period.

In general Q is a function of vibration amplitude, period, temperature, mechanical and thermal treatment, chemical impurity among other factors. For a given material, however, in a given physical state Q may be taken approximately as independent of the period. In porous media such as rocks, the dissipation is decreased by compression, resulting in an increase of Q with pressure.

From the values of γ given above and equation 5 we find

$$1/Q = 665 \times 10^{-5} \text{ for } T = 215 \text{ sec, } c = 4.5 \text{ km/sec}$$

$$1/Q = 673 \times 10^{-5} \text{ for } T = 140 \text{ sec, } c = 4.2 \text{ km/sec}$$

These may be compared to the values⁵ 1000×10^{-5} and 80×10^{-5} for Quincy granite at a pressure of 1 atmosphere and 4000 atmospheres respectively, obtained from laboratory studies of the logarithmic decrement of free vibrations at audio frequencies. The corresponding values for Vinal Haven diabase are 170×10^{-5} at 1 atmosphere and 280×10^{-5} at 4000 atmospheres. It is surprising that the values of internal friction determined in this way for the upper

5. See for example Birch, "Handbook of Physical Constants", Spec. Paper 36, Geol. Soc. Amer., 1942.

mantle is of the same order of magnitude as that found in the laboratory vibration measurements on crystalline rocks at audio frequencies.

Since depth of effective penetration of mantle Rayleigh waves increases with period, study of the variation of mantle structure with depth is feasible by this technique. Improved instrumentation will be required to extend the period range. Use of mantle Love waves (G waves) for which the penetration dependence on period varies differently may aid in the difficult problem of evaluating effects on Q of pressure and temperature of mantle rocks as well as wave periods.

DISCUSSION

Near the left side of Figure 8 are shown in full lines the dispersion curves for oceanic paths as given by Ewing and Press² and for continental paths as given by Wilaon and Baykal¹. These are theoretical curves which are well supported by observation. The oceanic curve is calculated for an ocean layer 5.57 km thick over an extended solid substratum with shear velocity $\beta_2 = 4.56$ km/sec, and density $\rho_2 = 3.0 \text{ gm/cm}^3$. The continental curve is calculated for a layer 37 km thick with $\beta_1 = 3.7 \text{ km/sec}$, overlying an extended substratum with $\beta_2 = 4.45 \text{ km/sec}$, and $\rho_2/\rho_1 = 57/50$. The theoretical extensions of the continental and oceanic dispersion curves to periods longer than those for which observations have been available approach the value $.92\beta_2$. These theoretical extensions assume that the substratum extends to infinite depth without change of properties. Under these conditions the asymptotic value of group velocity for long waves is about 4.2 km/sec. The asymptotic value is approached for shorter periods by the oceanic curve, than by the continental curve, the controlling layer being much thinner for the former case. But for periods greater than about 60 sec the two curves are approximately the same.

The marked deviation from these extended theoretical curves shown by the observations reported here of group velocity for longer periods is simply due to the fact that the long waves are reaching to depths where a change in the properties of the substratum is encountered. It will be shown by an approximate calculation that the necessary change in properties of the mantle, and the long period Rayleigh waves will be referred to as mantle Rayleigh waves to distinguish them from the shorter period crustal Rayleigh waves.

The period range between 40 sec and 70 sec is lacking in observations and corresponds to the transition from crustal to mantle propagation. The 70 sec curves which mark the short wave limit for mantle propagation are considered to be the shortest waves which are free from strong scattering and refraction at the major crustal discontinuities between oceans and continents, hence the absence of shorter periods from the higher order paths is expectable.

The absence of longer periods from R1 and R2 is a less definite matter. It is related to masking by the crustal Rayleigh waves to which the instruments are more sensitive and to the distance required for adequate spreading of the wave train.

Two layer approximation.

The calculations for a theoretical Rayleigh wave dispersion curve for periods up to 7 minutes for the known velocity and density distribution in the crust and mantle down to 1500 kilometers are

prohibitive if present methods are used, the principal complication arising from the gradual increase of velocity with depth.

The inverse problem of calculating the velocity depth relation from the dispersion observations is even more difficult.

As a first approximation a greatly simplified structure which is suggested by a calculation of Pekeris³ will be assumed.

Pekeris chose two liquid layers with thicknesses h_1 and h_2 over an extended liquid substratum and obtained the appropriate dispersion curve. He made two auxiliary calculations a) a single layer case in which h_2 is infinite, b) a single layer case in which h_1 is absent and found that, by virtue of the large ratio $h_2/h_1 = 10$, the three layer problem may be adequately represented by these separate single layer problems, greatly simplifying the calculations.

This suggests that crustal and mantle Rayleigh wave observations may likewise be represented by two separate single layer problems as follows:

(1) The continental or oceanic crust will be represented by a single homogeneous layer underlain by a homogeneous mantle of infinite extent, being the same in all respects as the previous solutions for crustal Rayleigh waves as shown at the left side of Figure 8 .

A still better approximation would make use of the recent treatment by Newlands⁶ of Rayleigh waves in a two layer heterogeneous medium with different values of the elastic parameters in order to secure a better fit with observed dispersion than she was able to.

6. Margery Newlands, "Rayleigh Waves in a Two-layer Heterogeneous Medium," Mon. Not. Roy. Astron. Soc., Geoph. Suppl. 6, 109-128, 1950.

(2) The mantle, in which it is known from body wave studies that the velocity increases gradually with depth, is approximated as a single layer problem with the constants $\beta_2 = 6.15 \text{ km/sec}$, $\alpha_2 = 10.93 \text{ km/sec}$, $\beta_1 = 4.48 \text{ km/sec}$, $\alpha_1 = 8.11 \text{ km/sec}$, $\rho_2/\rho_1 = 1.11$, $H = 516 \text{ km}$. The dispersion curve for this layering may be obtained from the computations by Haskell⁷ for Rayleigh wave propagation in multi-layered media. The value of β_1 was taken to be close to that derived for the substratum in the studies of crustal Rayleigh waves. H was selected to make the period of the point of minimum group velocity coincide with the observed Airy phase (225 sec and 3.54 km/sec). The calculated dispersion curve is shown in Fig. 8. The curve is not a good fit, but it shows that the general trend of the observed curve can be explained as a minimum of group velocity caused by increase of shear wave velocity with depth in the mantle. It is considered probable that a better fit could be obtained if calculations were available for a structure resembling the actual mantle more closely. Again the results of Newlands could be used to compute better approximations.

Referring to Figure 11, where the velocity-depth curve of Gutenberg is shown, it is seen that the velocity-depth relation deduced from the highly simplified one layer dispersion calculation is in reasonably good agreement.

7. Norman Haskell, "The Dispersion of Surface Waves on Multi-Layered Media", Geophysical Research Paper No. 6, Air Force Cambridge Research Center.

CONCLUSIONS

An investigation of mantle Rayleigh waves from three earthquakes has resulted in a group velocity curve with data from R2, R3, R4, R5, R7 waves showing surprisingly little scatter. The group velocity curve has a definite minimum value at a period of 225 sec and velocity of 3.54 km/sec. It is suggested that the known variation of shear wave velocity with depth in the mantle can account for the observed dispersion. The small scatter in velocity for the large range of distances and the different paths indicates that the scattering and refraction effects at continental margins and differences between oceanic and continental crustal structure have no influence on the propagation of these waves. For this reason the value of $1/Q=670 \times 10^{-5}$ deduced for the internal friction in the upper mantle for waves of periods 140-225 sec is believed to be a fairly accurate determination.

TABLE I

R₃ Arrival Times for Maximum Trace Deflection 15 Aug. 1950

Uncorrected			Uncorrected		
Phase	Arrival Time	Ground Ampl. mm	Phase	Arrival Time	
Short Period Branch			Long Period Branch		
U	17:59:38	G. C. T.	R	17:39:04	G. C. T.
C	18:00:02		C	41:50	
D	00:18		R	44:24	
R	00:40		C	47:20	
U	00:50		R	51:14	
C	01:17		C	53:25	
D	01:37		R	56:20	
R	02:14		C	58:32	
U	02:22		R	18:01:16	
C	03:12		C	03:55	
D	03:25	.36	R	06:00	
S	03:51		C	09:00	
R	04:02				
U	04:21	.44			
N	04:43				
C	05:00				
D	05:19	.82			
S	05:38				
R	06:04				
U	06:22	.94			
N	06:43				
C	07:18				
D	07:32	1.3			
S	07:57				
R	08:31				
U	08:43	1.5			
N	09:16				
C	09:50				
D	10:04	3.0			
S	10:43				
R	11:20				
U	11:32	4.2			
N	12:28				
C	13:00				
D	13:12	4.2			
S	14:12				
R	14:44				
U	15:02	3.6			
N	15:49				
C	16:28				
D	16:37				
S	17:27				
U	18:30				
D	20:25				

TABLE II

R₄ Arrival Times for Maximum Trace Deflection 15 Aug. 1950

Uncorrected			Uncorrected		
Phase	Arrival	Ground	Phase	Arrival	Time
	Time	Ampl. mm.			
Short Period Branch					
C	19:15:36	G. C. T.	R	18:40:00	G. C. T.
R	16:28		C	43:16	
C	17:36		R	47:00	
D	17:35	.38	C	49:40	
R	18:46		R	53:00	
U	18:54	.44	C	55:38	
C	19:54		R	58:20	
D	20:14	.44	C	19:01:04	
R	21:16		R	04:00	
U	21:16	0	U	03:48	
C	22:38		C	06:26	
D	22:37	.68	D	06:36	
N	23:06		R	08:54	
R	23:52		U	09:25	
U	24:17	1.7	C	11:52	
S	24:56		D	12:17	
C	25:34		R	14:08	
D	25:53	2.8	U	14:12	
N	26:32		C	16:36	
R	27:24		R	18:40	
U	27:40	2.2	C	21:20	
S	28:21				
C	29:28				
D	29:21	1.5			
N	30:21				
U	31:46	.8			
S	32:43				
D	33:21				
N	34:36				
S	36:44				

TABLE III

R₅ Arrival Times for Maximum Trace Deflection 15 Aug. 1950

Uncorrected			Uncorrected		
Phase	Arrival Time	Ground Ampl. mm.	Phase	Arrival Time	
Short Period Branch			Long Period Branch		
D	21:07:10	G. C. T.	R	20:33:13	G. C. T.
U	08:07	.16	C	35:36	
D	09:03	.18	R	38:32	
U	10:23	.26	C	41:32	
N	11:08		R	44:16	
C	11:45		C	47:00	
D	11:55	.28	R	49:28	
S	12:45		U	49:30	
R	12:47			N	52:12
U	13:16	.30	C	52:36	
N	14:08		D	52:36	
C	14:07		S	54:25	
D	14:26	.32	R	55:38	
S	15:09		U	55:54	
R	15:40			N	56:36
U	15:44	.76	C	57:30	
N	16:23		D	58:28	
C	17:22		S	59:04	
D	17:15	1.0	R	59:20	
S	18:13		U	21:00:32	
R	18:50			N	01:28
U	19:06	1.2	C	02:00	
N	20:03		D	02:38	
C	20:28		S	04:15	
D	20:55	1.3	R	04:36	
S	21:50		U	04:49	
R	22:44			N	06:50
U	22:50	1.4	C	07:28	
N	23:09		D	07:10	
D	24:34	.74	R	09:50	
S	25:31		C	11:44	
N	27:09				

TABLE IV

R₇ Arrival Times for Maximum Trace Deflection 15 Aug. 1950

Phase	Uncorrected Arrival Time	Ground Ampl. mm.
U	24:23:04 G. C. T.	
	D 24:52	.60
U	26:54	.60
	D 28:48	.60
U	30:25	
	D 32:12	
U	34:09	

TABLE V

Dispersion Data for R₃, R₄, R₅, R₇ 15 Aug. 1950

		R ₃	$\Delta = 52,210 \text{ km}$		
Uncorrected Time *	Period in sec		Travel Time h:m:s	Travel Time in sec	Velocity in km/sec
17:42:00	G. C. T. 370		03:32:53	12,773	4.09
17:50:10	344		03:41:03	13,263	3.94
17:57:30	316		03:48:23	13,703	3.81
18:04:00	292		03:54:53	14,093	3.70
18:09:10	274		04:00:03	14,403	3.62
18:13:20	240		04:04:03	14,643	3.57
18:17:50	226		04:08:43	14,923	3.50
18:18:00	220		04:08:53	14,933	3.50
18:14:10	212		04:05:03	14,703	3.55
18:11:00	190		04:01:53	14,513	3.60
18:08:30	158		03:59:23	14,363	3.64
18:06:20	132		03:57:13	14,233	3.67
18:04:20	120		03:55:13	14,113	3.70
18:02:30	102		03:53:23	14,003	3.73
18:00:50	86		03:51:43	13,903	3.76
17:59:50	69		03:50:43	13,843	3.77

		R ₄	$\Delta = 67,890 \text{ km}$		
Uncorrected Time *	Period in sec		Travel Time h:m:s	Travel Time in sec	Velocity in km/sec
18:43:30	G. C. T. 402		04:34:23	16,463	4.12
18:50:10	360		04:41:03	16,863	4.03
18:57:00	338		04:47:53	17,273	3.93
19:04:30	312		04:55:23	17,723	3.83
19:12:10	296		05:03:03	18,183	3.73
19:19:20	274		05:10:13	18,613	3.65
19:25:20	248		05:16:13	18,973	3.58
19:31:50	240		05:22:43	19,363	3.51
19:32:10	232		05:23:03	19,383	3.50
19:27:40	224		05:18:33	19,113	3.55
19:24:20	208		05:15:13	18,913	3.59
19:22:00	158		05:12:53	18,773	3.62
19:20:00	142		05:10:53	18,653	3.64
19:17:50	136		05:08:43	18,523	3.67
19:16:20	124		05:07:13	18,433	3.68

TABLE V (cont'd.)

R_5 $\Delta = 92,240 \text{ km}$

Uncorrected Time *	Period in sec	Travel Time h:m:s	Travel Time in sec	Velocity in km/sec
20:38:00 G. C. T.	342	06:28:53	23, 333	3.95
20:49:00	320	06:39:53	23, 993	3.84
20:59:30	290	06:50:23	24, 623	3.75
21:08:30	276	06:59:23	25, 163	3.67
21:15:30	264	07:06:23	25, 583	3.61
21:21:10	244	07:12:03	25, 923	3.56
21:25:20	228	07:16:13	26, 173	3.52
21:25:20	220	07:16:13	26, 173	3.52
21:20:50	216	07:11:43	25, 903	3.56
21:17:00	192	07:07:53	25, 673	3.59
21:14:30	168	07:05:23	25, 523	3.61
21:12:00	158	07:02:53	25, 373	3.64
21:10:05	148	07:00:58	25, 258	3.65
21:08:40	131	06:59:33	25, 173	3.66
21:07:40	108	06:58:33	25, 113	3.67

R_7 $\Delta = 132,270 \text{ km}$

Uncorrected Time *	Period in sec	Travel Time h:m:s	Travel Time in sec	Velocity in km/sec
24:28:40 G. C. T.	223	10:19:33	37, 173	3.55

*Clock correction + 23 sec.

TABLE VI

Arrival Times for Maximum Trace Deflections
2 March 1933

Uncorrected		Uncorrected	
R2	Arrival	R3	Arrival
Phase	Time	Phase	Time
Short Period Branch			
C	11:48:10 P.S.T.	C	13:05:33 P.S.T.
R	48:48	R	13:06:34
C	49:43	C	07:35
R	50:33	R	08:40
C	51:12	C	09:45
R	51:46	R	11:06
C	52:32	C	12:21
R	53:26	R	13:28
C	54:19	C	15:00
R	55:23	R	16:40
C	56:29	C	19:06
R	57:45		
C	59:06		
R	12:00:54		
C	12:02:25		
R	12:04:43		

Uncorrected	
R4	Arrival
Phase	Time
Short Period Branch	
R	15:01:53 P.S.T.
C	15:03:22
R	15:05:10
C	15:06:52
R	15:09:11

TABLE VII

Dispersion Data 2 March 1933

R2

Uncorrected Arrival Time *	Period in sec.	Travel Time in sec.	Velocity in km/sec.
11:52:10 P. S. T.	96.5	8457	3.76
53:08	106	8515	3.73
54:00	112	8567	3.71
55:00	124	8627	3.69
56:10	133	8697	3.66
57:20	154.5	8767	3.63
59:10	189	8877	3.58
12:01:35	225	9022	3.52

R3

13:06:00 P. S. T.	120	12887	3.75
13:07:30	126	12977	3.72
13:08:55	138	13062	3.70
13:10:25	144	13212	3.65
13:12:10	158	13257	3.64
13:13:55	176	13362	3.61
13:15:40	206	13467	3.58
13:17:30	232	13577	3.55

R4

15:02:50 P. S. T.	192	19897	3.61
15:05:10	220	20037	3.58
15:07:55	252	20202	3.56

* Clock correction -12 sec

TABLE VIII

R2 Arrival Times and Dispersion Data for 8 Sept. 1948

$$\Delta = 31,470 \text{ km}$$

Phase	Uncorrected*		Uncorrected*		Travel	
		Time	Arrival Time	Period in sec.	Time in sec.	Velocity in km/sec.
G. C. T.						
U			17:25:25	59	8178	3.85
	D	17:25:05	17:26:50	90	8263	3.81
U		25:35	17:29:20	113	8413	3.74
	D	26:10	17:32:05	136	8578	3.67
U		26:55	17:34:35	198	8728	3.61
	D	27:40				
U		28:35				
	D	29:35				
U		30:25				
	D	31:30				
U		32:40				
	D	34:05				
U		35:40				

* Clock correction + 7 sec.

TABLE IX

Ground Amplitudes for Various Periods 15 August 1950

R3 Short Period Branch

Ground	
T	Ampl. mm.
110	.40
131	.74
150	1.3
180	2.6
192	3.5
205	4.5
209	4.1
212	3.2
215	2.2

R4 Short Period Branch

Ground	
T	Ampl. mm.
138	.40
145	.48
160	.60
175	.76
202	1.4
217	2.8
225	2.1
230	1.3
233	.80

R5 Short Period Branch

Ground	
T	Ampl. mm.
122	.16
150	.28
160	.32
167	.36
178	.76
200	1.1
210	1.2
221	1.4
227	.74

R7

Ground	
T	Ampl. mm.
223	.60

CAPTIONS

Figure 1.... Tracings of the Pasadena N-S linear strain ($T_g=70$ sec), vertical and N-S ($T_0=1$ sec, $T_g=90$ sec) seismographs for the earthquake of 15 August 1950.

Figure 2.... Arrival time, period and amplitude curves for R3 waves from earthquake of 15 August 1950.

Figure 3.... Arrival time, period and amplitude curves for R4 waves from earthquake of 15 August 1950.

Figure 4.... Arrival time, period and amplitude curves for R5 waves from earthquake of 15 August 1950.

Figure 5.... Arrival time, period and amplitude curves for R7 waves from earthquake of 15 August 1950.

Figure 6.... Arrival time curves for R2, R3, R4 waves from earthquake of 2 March 1933.

Figure 7.... Arrival time curve for R2 waves from earthquake of 8 September 1948.

Figure 8.... Observed group velocity curve for mantle Rayleigh waves compared to theoretical curve based on single layer approximation.

Figure 9.... Vertical ground amplitudes (peak to peak) for short period branch of R3, R4, R5, R7 waves as a function of period for earthquake of 15 August 1950.

Figure 10.... Graph of logarithm of product of ground amplitude and dispersion factor to obtain constants A_0 , \bar{A}_0 and γ .

Figure 11.... Comparison of shear wave variation with depth according to Gutenberg and single layer approximation deduced from mantle Rayleigh wave dispersion.

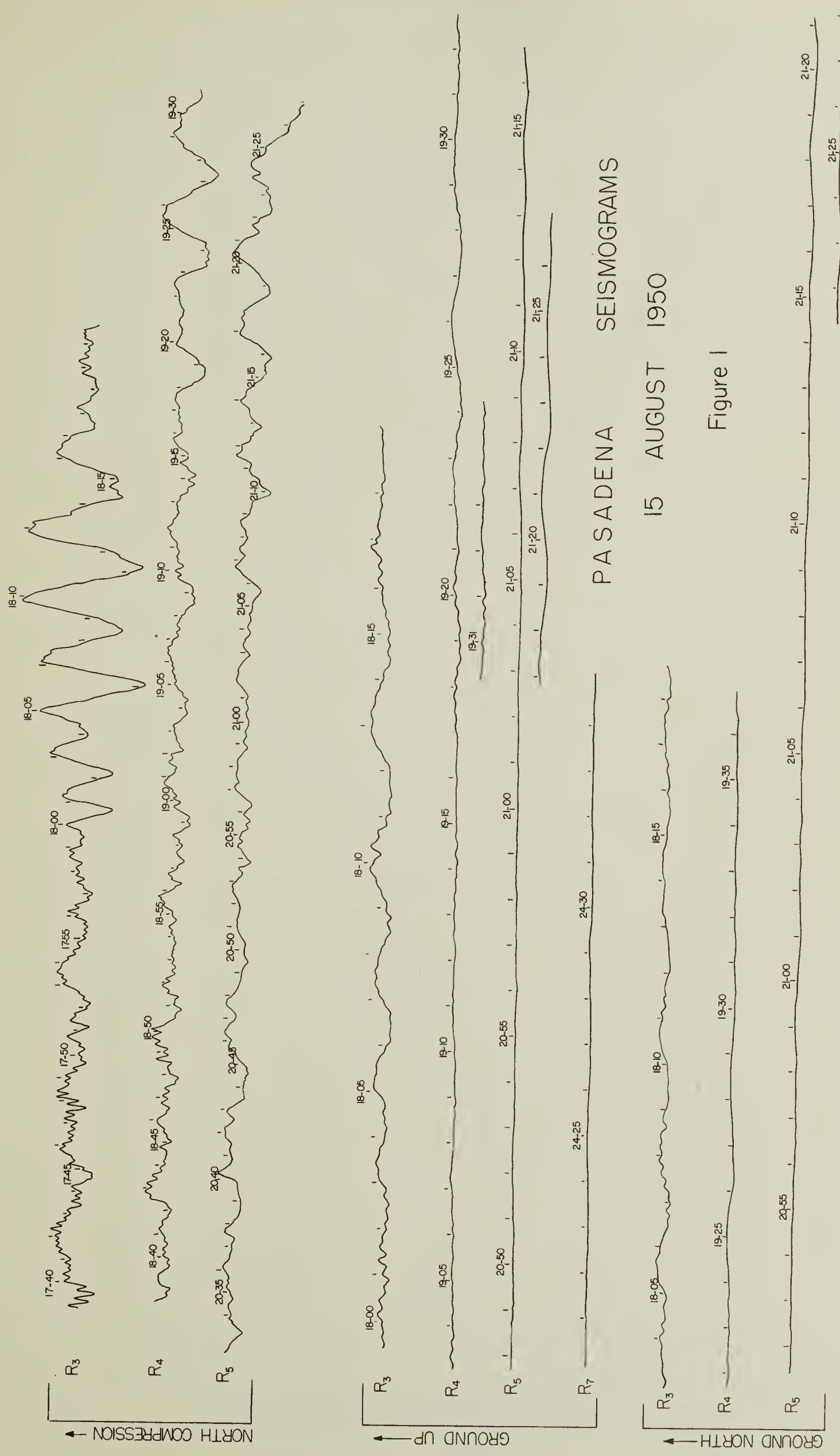


Fig. 2
 R_3 TRAVEL TIME, PERIOD,
 AMPLITUDE CURVES
 15 August 1950

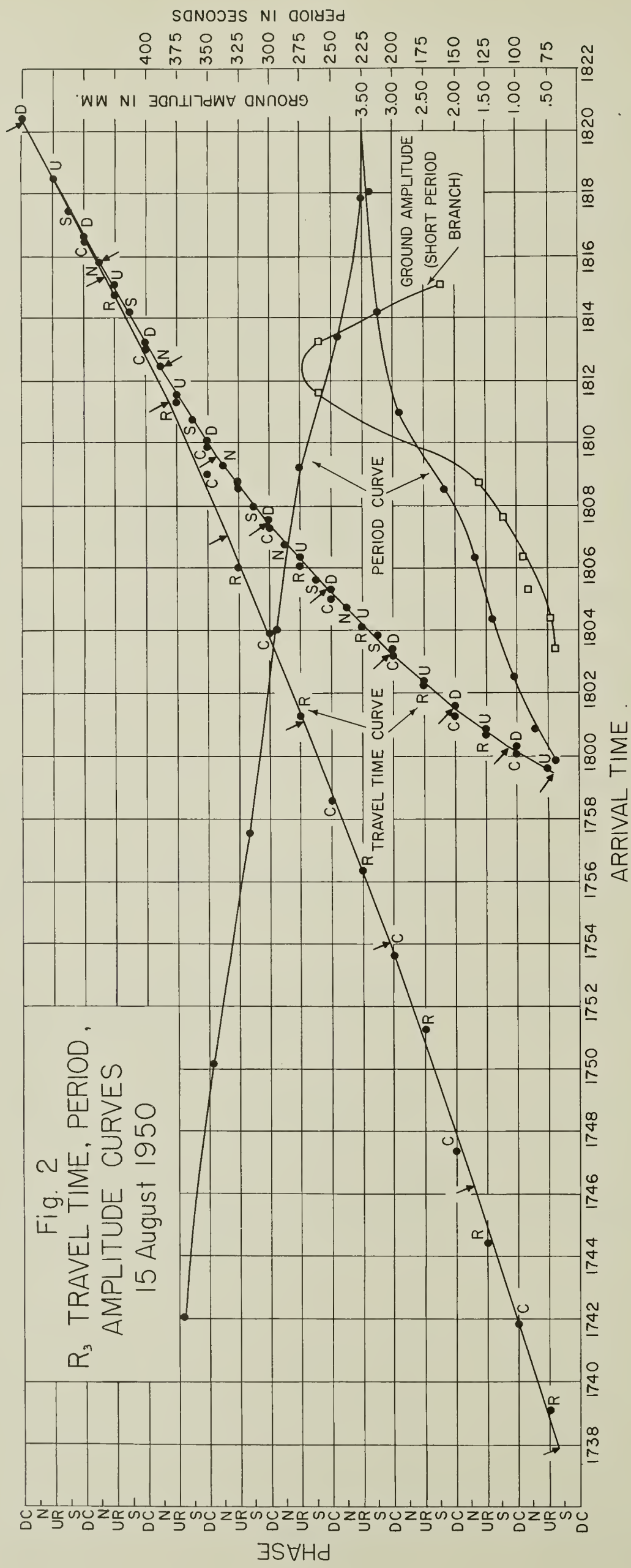
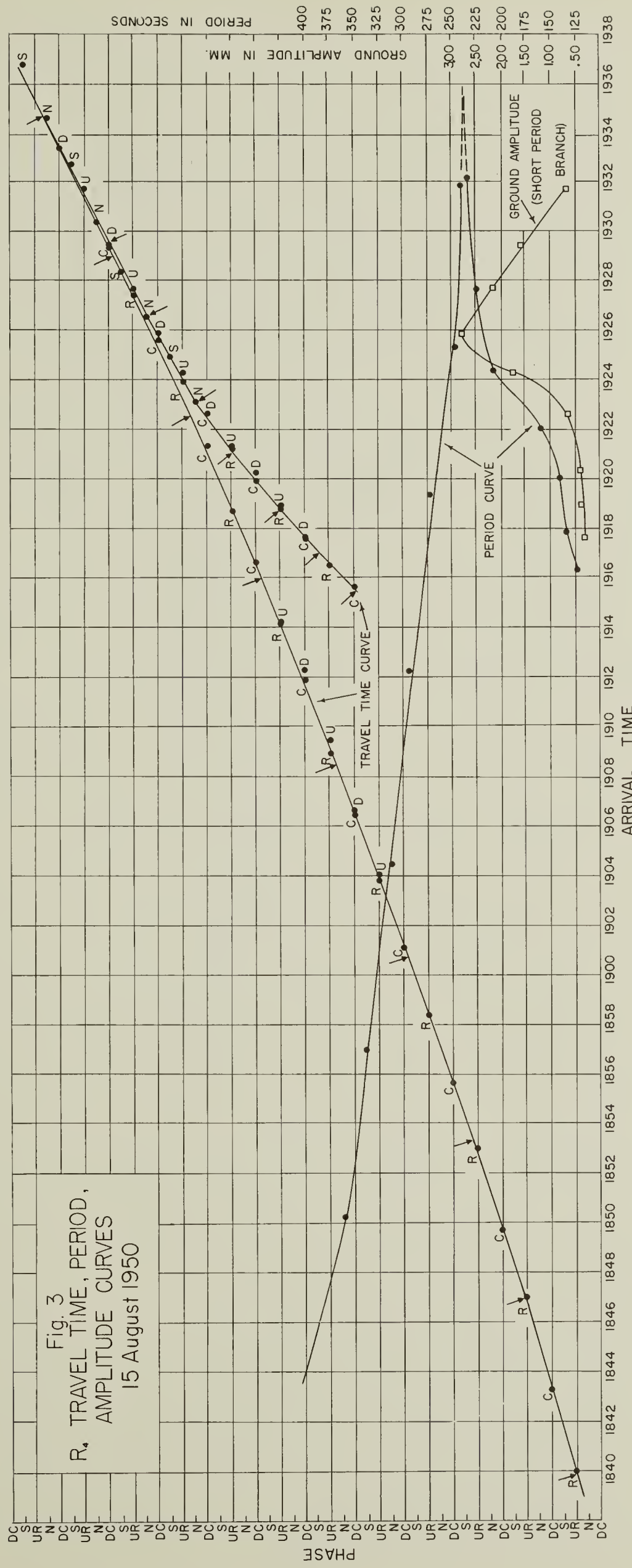
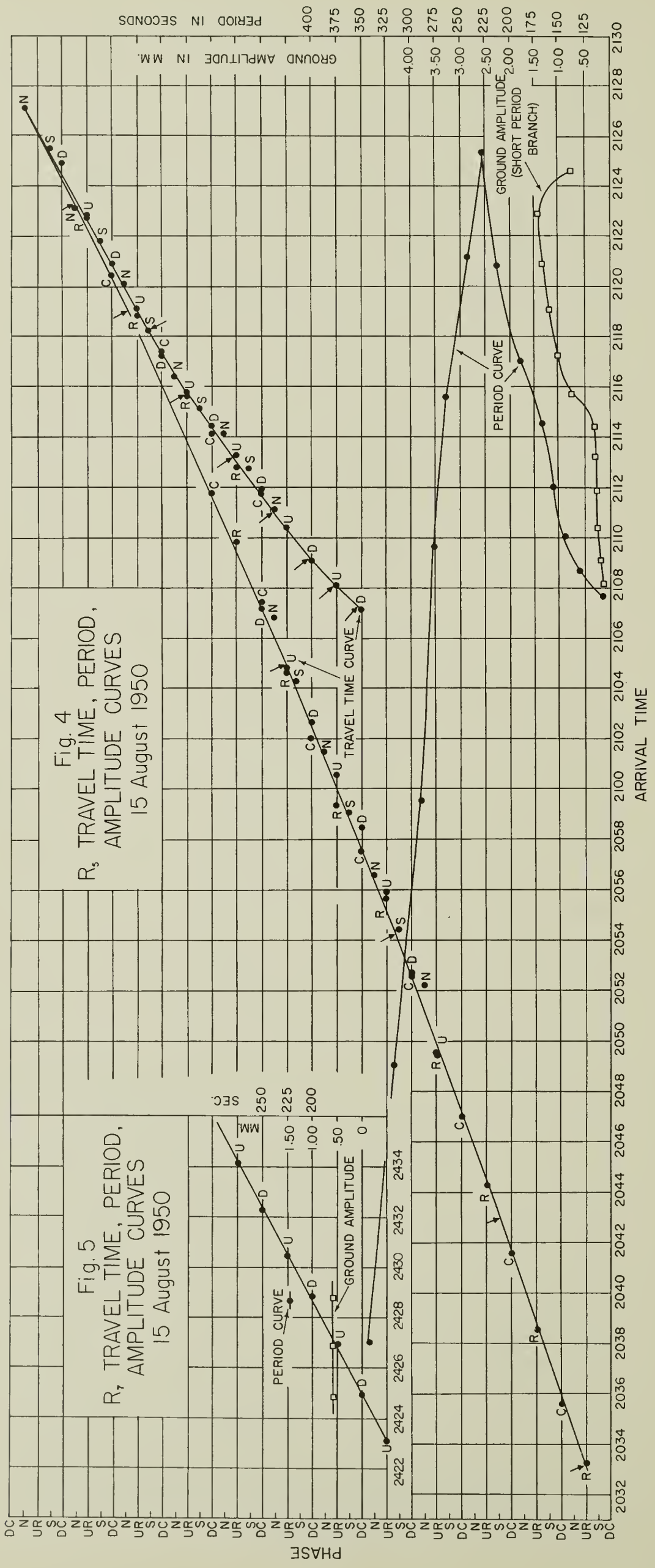
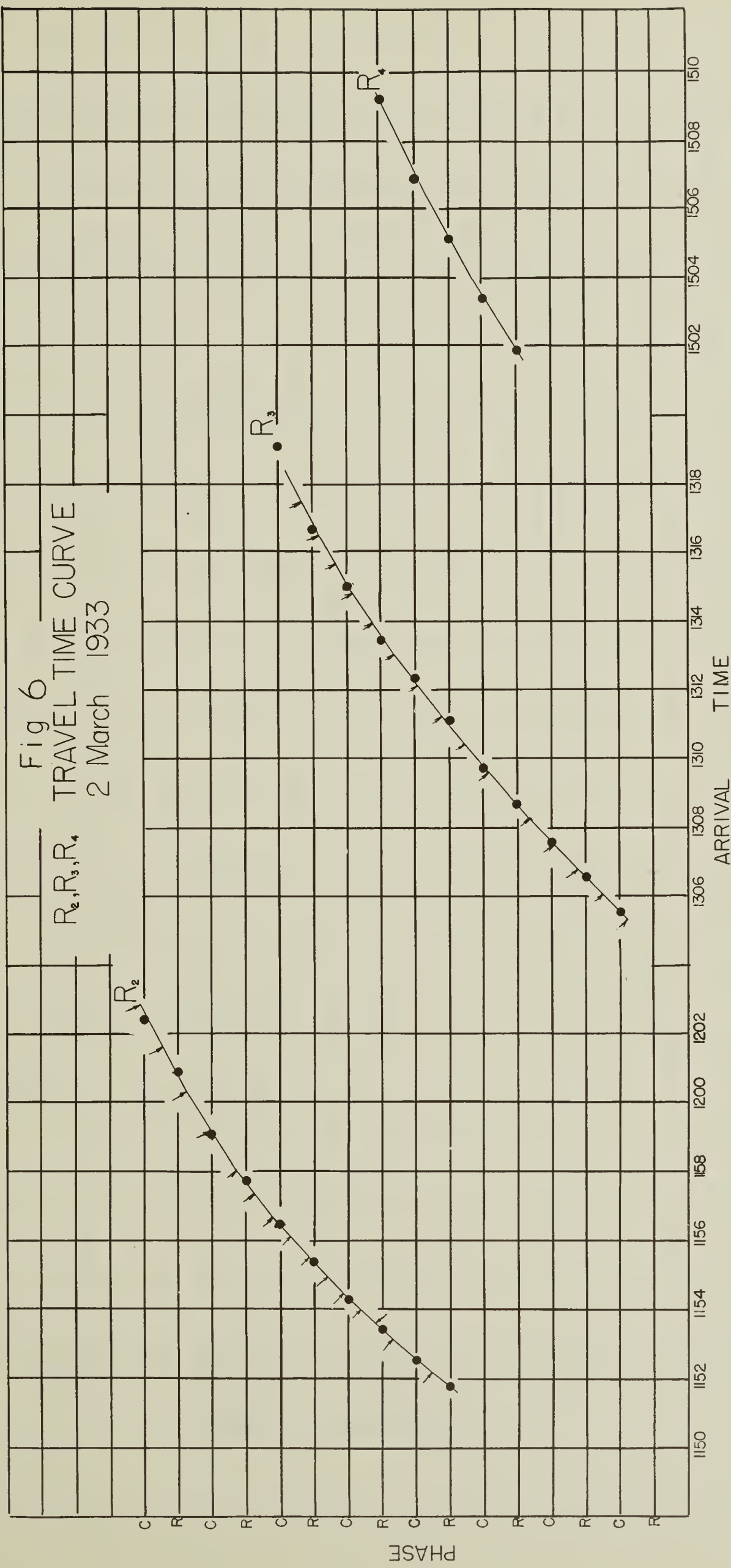


Fig. 3
R. TRAVEL TIME, PERIOD,
AMPLITUDE CURVES
15 August 1950







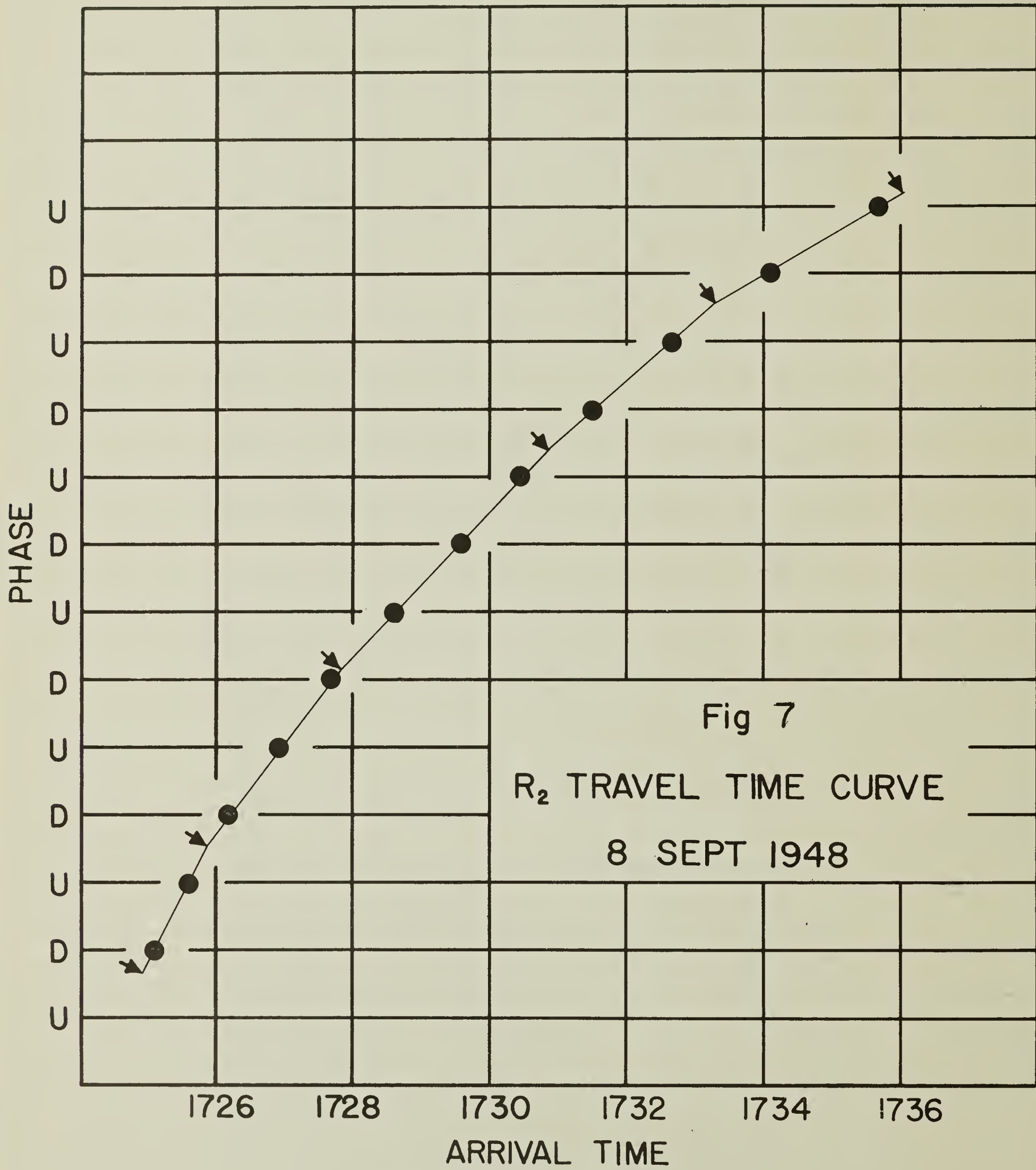


Fig 7

R₂ TRAVEL TIME CURVE

8 SEPT 1948

Fig. 8

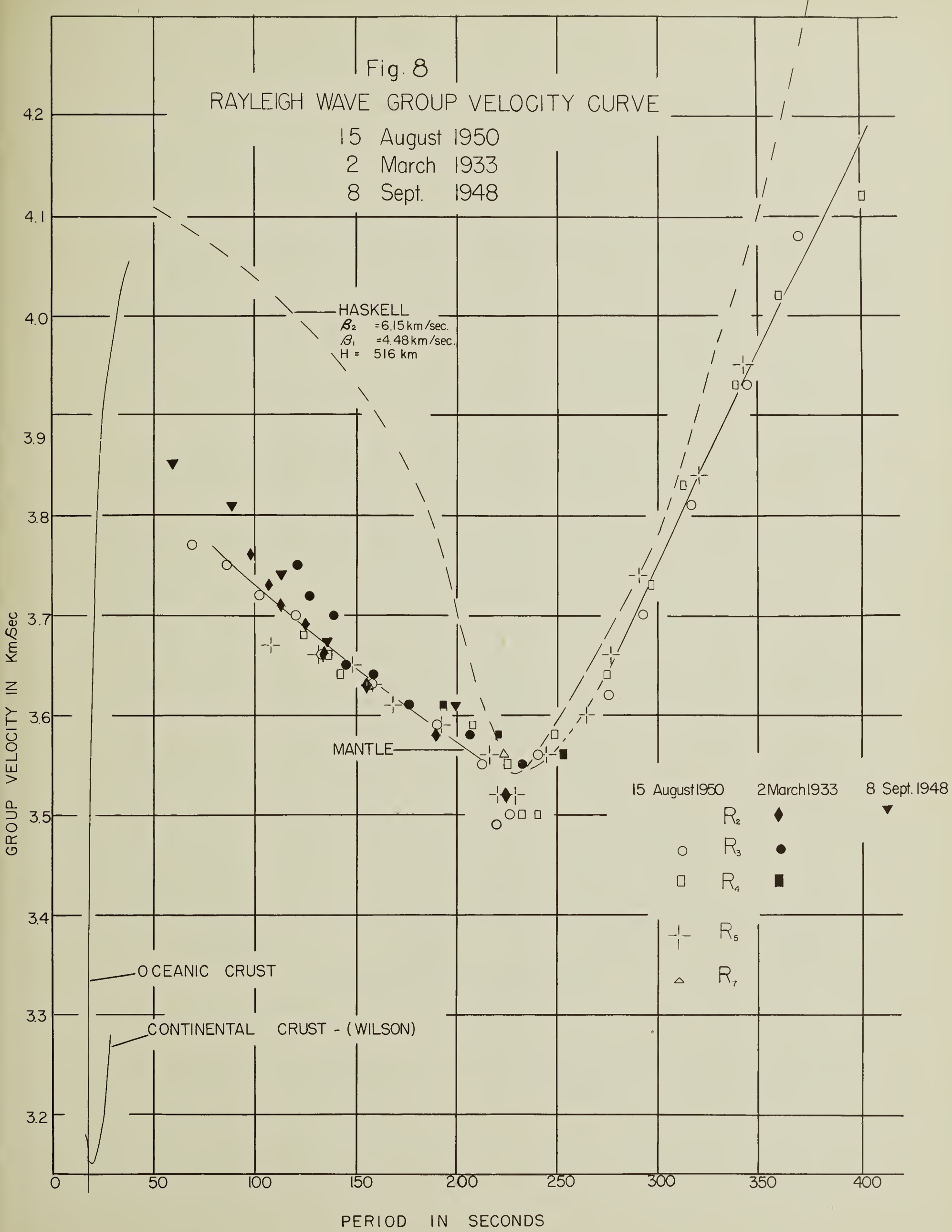
RAYLEIGH WAVE GROUP VELOCITY CURVE

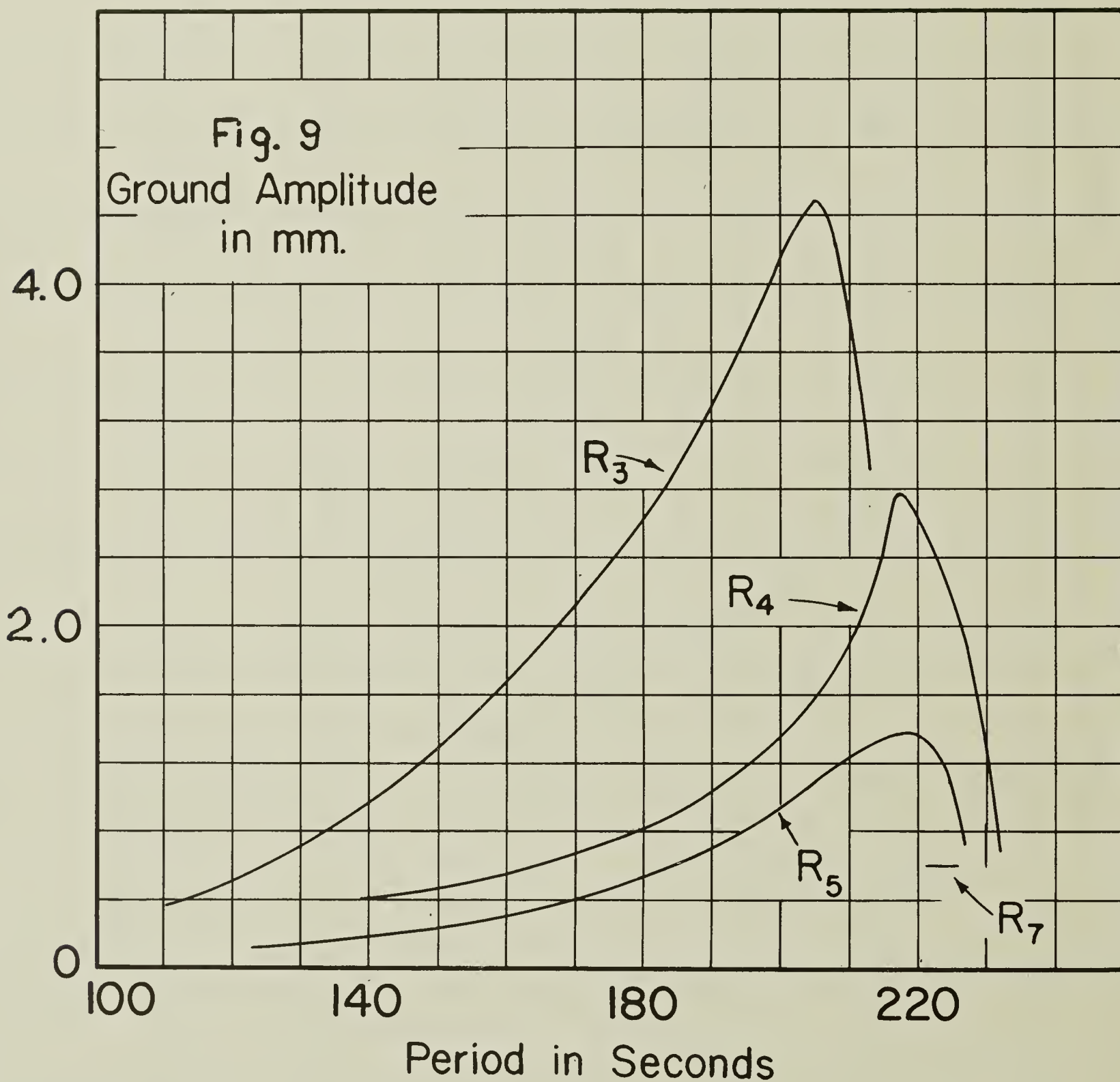
15 August 1950

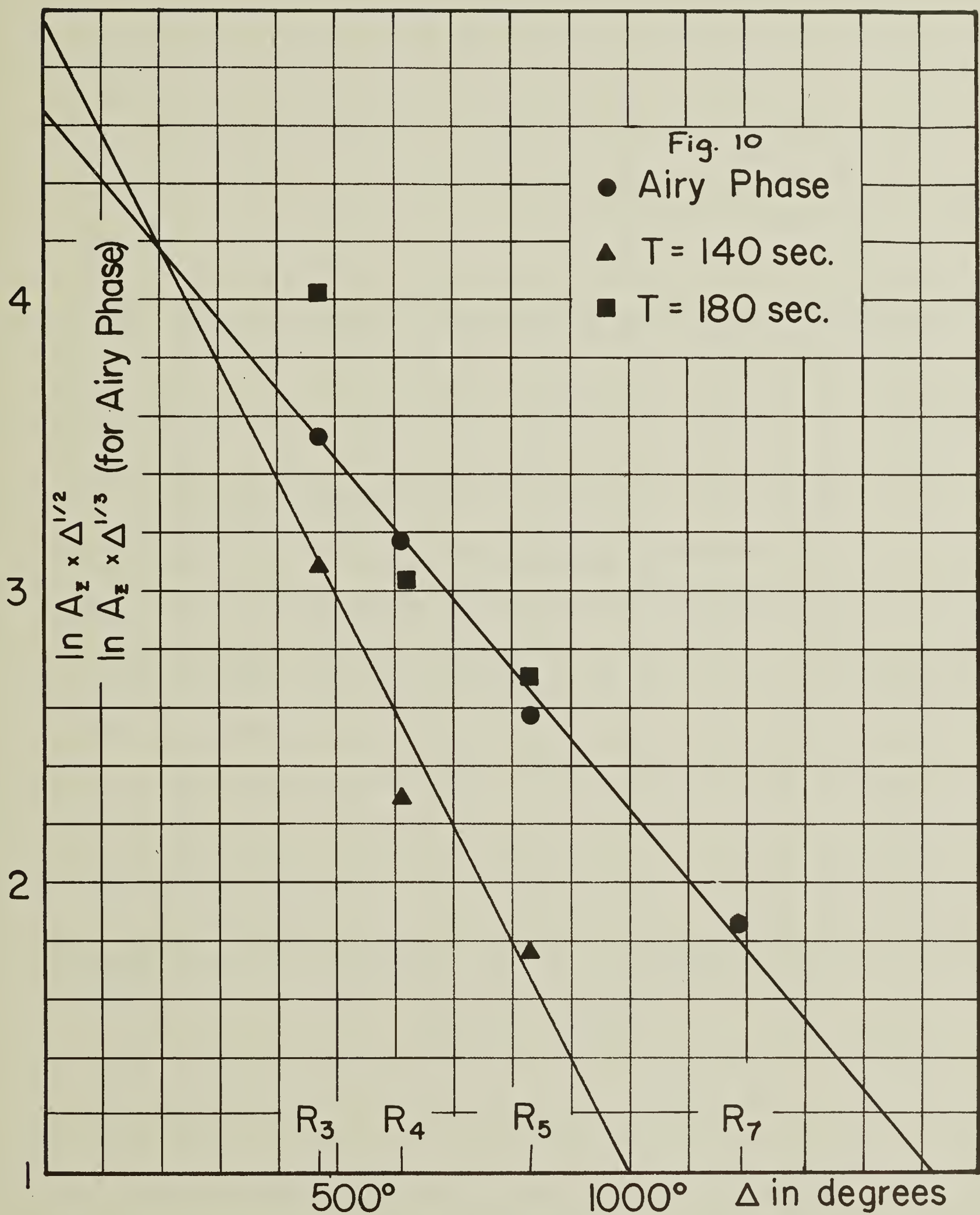
2 March 1933

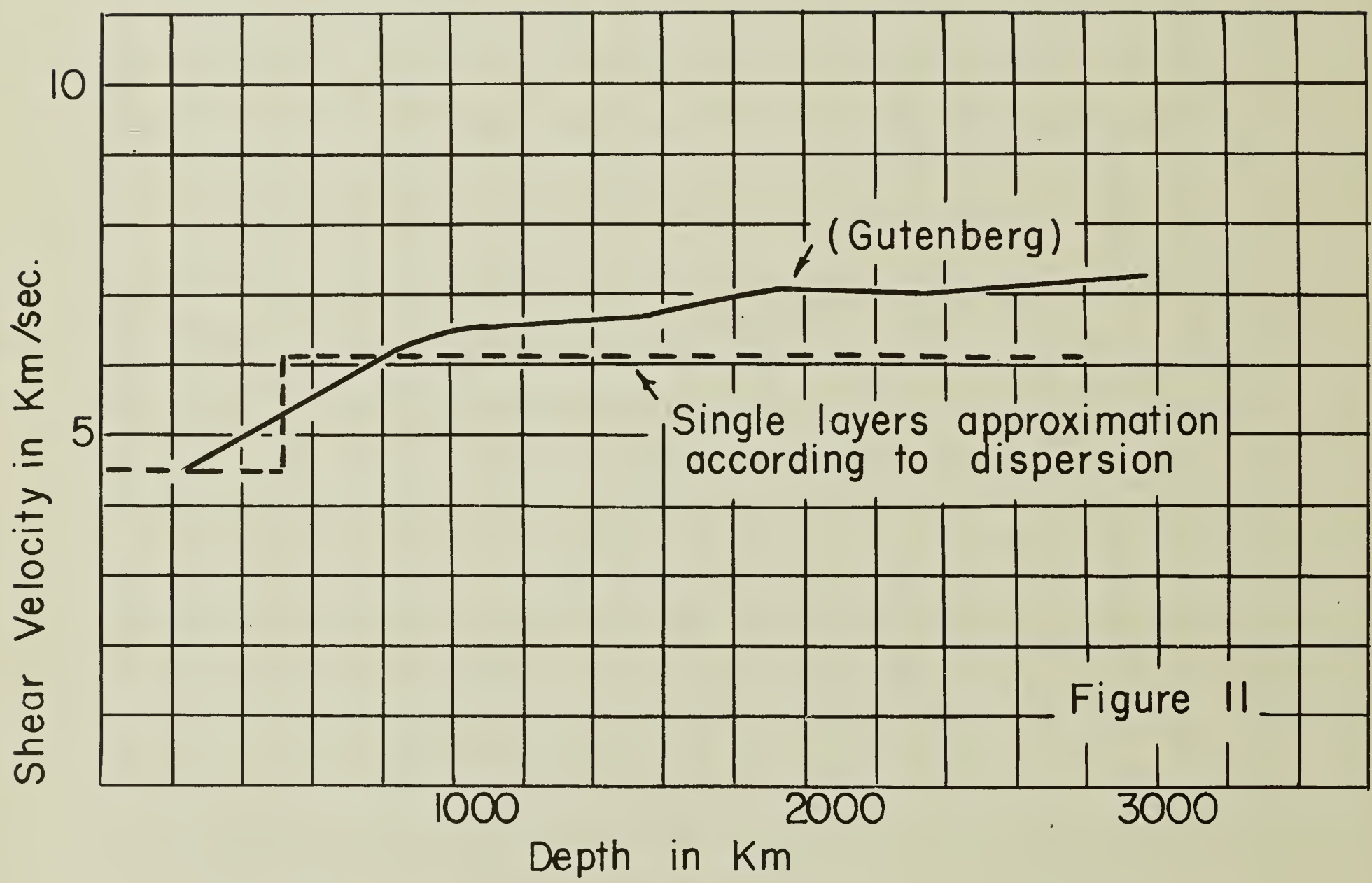
8 Sept. 1948

HASKELL
 $\beta_2 = 6.15 \text{ km/sec.}$
 $\beta_1 = 4.48 \text{ km/sec.}$
 $H = 516 \text{ km}$









COLUMBIA LIBRARIES OFFSITE



CU90645707

